

EMERGENCE OF THE SVD AS AN INTERPRETABLE FACTORIZATION IN DEEP LEARNING FOR INVERSE PROBLEMS

SHASHANK SULE, RICHARD G. SPENCER, AND WOJCIECH CZAJA

ABSTRACT. We demonstrate the emergence of weight matrix singular value decomposition (SVD) in interpreting neural networks (NNs) for parameter estimation from noisy signals. The SVD appears naturally as a consequence of initial application of a descrambling transform - a recently-developed technique for addressing interpretability in NNs [1]. We find that within the class of noisy parameter estimation problems, the SVD may be the means by which networks memorize the signal model. We substantiate our theoretical findings with empirical evidence from both linear and non-linear settings. Our results also illuminate the connections between a mathematical theory of semantic development [2] and neural network interpretability.

Interpreting the nature of the mapping between inputs and outputs of trained neural networks (NNs) remains one of the major unsolved problems in machine learning and is the focus of significant research effort [3, 4, 5, 6, 7, 8, 9, 10]. More recently, such efforts have succeeded in interpreting NN's in image classification by applying interpretation heuristics to the singular value decompositions (SVDs) of trained weights [1, 11, 12, 13]. The SVD has innumerable applications in statistics [14, 15], dimensionality-reduction [16, 17, 18], and geometric data science [19, 20]. It has also found previous application in specific deep learning settings, including sensing neural network topology [21], isotropic pattern recognition in control charts [22], neural network weight compression [23]. The key idea behind using SVD for NN interpretation is that the singular subspaces of NN-associated matrices, such as weight and data correlation matrices, encode the learning that occurs during training. This is particularly appealing when interpretation relies upon recognition of readily-identifiable patterns, such as *dog* or *cat* labels. Consequently, the hidden semantics of a trained NN may be uncovered by taking the SVD as a starting point and then applying a (possibly complicated) heuristic such as intertwiner groups [12] or hypergraph rearrangements [13] of these SVDs.

In this paper we show that this link between singular spaces and NN interpretation is more fundamental: an interpretation heuristic can be the starting point and the singular value decomposition can naturally emerge as an interpretation. We specifically exhibit this phenomenon for *smoothness descrambling transformations* - or simply, descrambling transformations - for interpretations of NNs used in signal processing [1]. Neural networks are routinely used for such regression problems in the sciences [24, 25, 26, 27] where network outputs are no longer simple class labels but are objects in a desired function space, and the network is trained to learn the underlying mapping between the input and output function classes. While these networks often match the prior state-of-the-art, their interpretability in the context of these problems remains an open question since the applicability of NN interpretation techniques from image classification is not established yet. To that end, we have focused on the SVD and the latent orthogonal transformations learned by the network motivated by the observation that many well-known transformations, such as the Fourier transform, are unitary and thus serve as a standard for human readability. This approach is quite promising: an analysis of linear two-layer neural networks [2] showed that the first and last weight matrices interact with the SVD of the covariance matrices from the distributions of training data. In particular, if the network structure is given by $f(x) = W_2 W_1 x$, then the weights W_1 and W_2 in the large data limit obey the continuous-time evolution law:

$$(1) \quad W_2(t) = U A(\Lambda, t) Q^{-1} \quad W_2(t) = Q A(\Lambda, t) V^\top$$

Here U and V are the right and left singular vectors of the input-output correlation matrix $\Sigma_{yx} = \mathbb{E}[yx^\top] = U \Lambda V^\top$. While this simple model shows that the singular vectors closest to both input and output data learn semantics from the data distribution, an understanding of the intermediate weight matrices (matrices of the type Q in (1)) and the case of nonlinear and deep networks, remains unresolved. A major step in addressing this problem was taken in [28], in the context of digital signal processing, where a fully-connected network

DEERNet was trained to solve the inverse problem of recovering a signal z from measurements of $s(z) + \alpha^{-1}y$ where s is a forward map and y is white noise with signal to noise ratio (SNR) α^{-1} . The hidden layer semantics of this network was interpreted in [1] through the introduction of descrambling transformations, which are also essential objects of our analysis. The basic idea of *descrambling* is to interrogate, or *wiretap*, the network's output F at the k th layer with a matrix P ((2)). P is then computed as the minimizer over a specified group G of well-chosen functionals η :

$$(2) \quad F = \sigma W_m \cdots \sigma P^{-1} \overbrace{P W_k \cdots W_1 X}^{f_k(P)}$$

$$(3) \quad \widehat{P}(k, X) = \operatorname{argmin}_{P \in G} \eta(f_k(P))$$

The motivation for choosing P to range over the representations of a group G is that any matrix P that successfully wiretaps a neural network represents an interpretable rearrangement of the nodes, and the composition of any two rearrangements should also be a rearrangement. This assumption leads naturally to a group structure on the search space of the minimization problem. *Smoothness criterion descrambling* is the specialization of (3) in which $\widehat{P}(k, X)$ is computed to promote smoothness of the intermediate data over the orthogonal group $O(n)$. The focus of this paper will be on smoothness criterion descramblers $\widehat{P}(k, X)$; we give a characterization of the MDS descrambling transformations in the [SI appendix](#).

The minimizers $\widehat{P}(k, X)$ defined in Equation 3 seek to transform the outermost weight matrices W_k into (visually) interpretable objects. For instance, descrambling analysis of the aforementioned DEERNet (a network used to solve a noisy Fredholm equation arising in electron-electron resonance) indicates that the network learns a variety of signal processing transformations such as a notch filter or a basis projection [1]. In this sense descrambling can extract the latent mathematical transformations learned by the network and expresses them in the well-known theoretical framework of digital signal processing.

Contribution. Prompted by these empirical results the goal in our paper is to analyse the theoretical properties of smoothness criterion descramblers $\widehat{P}(k, N)$ with a special focus on the case when the network F is trained to solve a noisy parameter estimation problem. Our main finding is that the SVD naturally emerges as a large data limit of these descrambling transformations: Theorem 1 shows that when the first layer of the network is wiretapped and the data is purely noisy the limiting descrambler matrix $\widehat{P}(1)$ can be written in terms of a trigonometric basis and the left singular vectors of the weight matrix W . In this way, we find an analogue of (1) for the matrices $\widehat{P}(1)$. We generalize this result to characterize the more realistic situation where the data $x = s(z) + \alpha^{-1}y$ is obtained as noisy measurements of a signal; in this case we show that the descrambler $\widehat{P}(1, X)$ promotes sinusoidality of the corresponding input/output signal library of the descrambled weight matrix and that the signal-to-noise ratio α^{-1} parameterizes a continuous path from the descrambler $\widehat{P}(1, X)$ and the identity matrix I . We also show that in the case when the wiretapped networks are non-linear the descrambler $\widehat{P}(k, N)$ is related to the SVD of the *Jacobian* of the wiretapped network at the empirical mean of the data X . The descrambler thus records not just the intrinsic properties of the SVD of the raw weights W but also the distribution of the data X . In this way we show that the choice of data model *matters* not only in training but also in interpretation via descrambling; in particular we show how the signal-to-noise ratio in the training data, which is independent of the NN, affects the descrambler matrix $\widehat{P}(k, X)$ (Theorem 2).

While the mathematics of our main results is interesting in its own right and will be discussed in the following sections, we highlight here three important consequences of our results, especially in light of prior experimental evidence. First, we observe that our results on the sinusoidality of descrambled weights give a theoretical account of the empirical results obtained for the descrambling analysis of DEERNet [1]: in particular we give a quantitative justification for why Fourier domain visualization yields intelligible representations of descrambled weights. Second, we show how descrambling can define classes of problem-dependent *interpretable* networks - networks where descramblers converge to the identity transformation - and how convolutional neural networks emerge as interpretable networks for certain inverse problems. Third, we find that descrambling wiretapped networks by feeding purely noisy data *still* allows for an interpretation of the weights – leading us to conjecture that the forward map is “memorized” in the right singular vectors of the first weight matrix, without necessarily memorizing instances of training data. We confirm this conjecture empirically in two different examples of noisy signal recovery–DEER spectroscopy

and biexponential parameter estimation—noting that right singular vectors of the first weight matrix closely resemble the training data model independently of the descrambling.

1. SMOOTHNESS CRITERION DESCRAMBLING

In this section we formulate the main mathematical problem that we address in this paper. Let η – the objective function, be the descrambler criterion and let \hat{P} denote the descrambler. The goal of this procedure is design η which yields a simple, human readable explanation of the descrambled weight matrices $P^*(k, X)W_k$. In this context the *smoothness criterion*

$$(4) \quad \eta(P) = \|D^2 PW_k \circ \sigma \circ \cdots W_1 X\|_F^2$$

is well suited for interpretation of linear layers of feedforward networks. The motivation behind this criterion is that while the network’s incoming and outgoing data is usually smooth and has an intelligible time-ordered structure, the intermediate data often loses this structure. As such, the role of the descrambler is to change basis so that the intermediate signal is itself smooth — and thus ordered with respect to the indices of the output or input dimension. This strategy was used successfully to interpret the first layer of DEERNet [1, 28]. Our goal is to study the minimizers

$$(5) \quad \hat{P}(k, X) := \operatorname{argmin} \|DPf_k(X)\|_F^2 \quad \text{w.r.t } P^\top P = I.$$

Here X denotes the matrix of the training data, which we assume is drawn from a context-dependent prior distribution. Different choices of this prior will lead to different solutions of the descrambling problem 3. However, for any general prior it is difficult to say anything about the structure of $\hat{P}(k, X)$. As a consequence we focus on the case where X models data used in inverse problems – the original use-case of descrambling transformations. Thus each column of X can be written as a noisy measurement $s(z) + \alpha^{-1}y$ where z is a to-be-recovered variable, y is noise, and α^{-1} is the SNR. We will first understand the case when the network is linear and the input is only noise. Then we will generalize it to the case where the output has an underlying signal, and finally when the network is non-linear. All proofs have been outlined in the [SI appendix](#).

2. RESULTS

We proceed to characterize the minimizers of (5) – the smoothness criterion descrambling problem. As stated above, the minimizer $\hat{P}(k, X)$ depends on the matrix X and the wiretapped network f_k . Our main mathematical innovation is to separate the cases $k = 1$ (when f_k is affine) and $k \geq 2$ to consider X as sampled over a distribution. This enables us to model the real-life settings in which neural networks are trained and evaluated. With these assumptions in mind, we state our main theoretical results below.

Linear Network, Only Noise. We first address the case when $k = 1$ in (5). In this case, $f_1(x) = W_1 x$ so the wiretapped network f_1 is linear. Additionally, to approach the data models present in inverse problems, we first consider the case where X is pure noise, i.e $x_i \sim \xi$ where ξ is some isotropic random variables. The canonical example of such a random variable is if $\xi \sim N(0, I_d)$. Our strategy to understand the minimizers of (5) is to study the convergence of \hat{P} as $N \rightarrow \infty$. As such, we denote $\hat{P}(k, X_N) := \hat{P}(N)$ and $X := X_N$ to keep track of the number of data points and implicitly assume $k = 1$. We shall see that these minimizers $\hat{P}(N)$ have a limit \mathcal{P} given by the (strong) law of large numbers (SLLN). However, to use the SLLN to swap a limit and a minimum we need to ensure the stability of the singular spaces of the random matrices WX_N . Bearing this in mind we first introduce the following definition.

Definition 1. Let $A_{n,m} \subseteq M_{n,m}(\mathbb{R})$ be the set of matrices with distinct non-zero singular values. Let $A = \bigcup_{n,m} A_{n,m}$ be the set of *admissible matrices*. A fully-connected feedforward NN with weights $W_k \in A$ is termed an *admissible neural network*.

Using the definition of admissibility, the following lemma can be proved using the continuity of the simple eigenvalues of a matrix in its entries [29]:

Lemma 1. Let W_n be a sequence of matrices such that $W_n \rightarrow W$ in the Frobenius norm, where $W \in A$. Then, the left and right singular vectors $\{u_i^n\}$ and $\{v_i^n\}$ of W_n converge to the right and left singular vectors of W , respectively.

Henceforth, we shall only work with admissible neural networks. Note that since $A_{n,m}$ is a dense subset of $M_{n,m}$, admissible neural networks are dense in the set of neural networks. Note that for $k = 1$, we can simplify (5) to

$$(6) \quad \widehat{P}(N) = \operatorname{argmin} \|DPW_1X_N\|_F^2 \quad \text{w.r.t } P^\top P = I.$$

We make the following assumptions modelling the empirical setup in [1]:

- (1) D is a Fourier Differentiation Stencil
- (2) X is a random $d \times N$ matrix such that each column x_i is drawn independently from a zero-mean isotropic density.
- (3) T is the $m \times m$ matrix such that every k th column has l th entry $t_k(l)$ given by

$$t_k(l) = \begin{cases} \cos \frac{\pi lk}{m} & k = 2n \\ \sin \frac{\pi l(k+1)}{m} & k = 2n - 1. \end{cases}$$

With these assumptions we can show that as the number of points N tends to infinity, $\widehat{P}(N)$ can be expressed in terms of the matrix T and the SVD of W_1 :

Theorem 1. Let f be an admissible NN with W_1 as its first layer weight matrix with rank- r SVD $W = U_r\Sigma_r V_r^\top$. Additionally, let T_r be the matrix formed by selecting the first r columns of T . Then,

$$(7) \quad \widehat{P}(N) \longrightarrow \widehat{\mathcal{P}} := T_r U^\top \text{ a.s. with } N \rightarrow \infty.$$

In particular, the descrambled weight matrix converges to $T_r \Sigma V^\top$ almost surely in the measure induced by x .

Thus, under certain geometric assumptions for the data X (isotropic, finite second moment), weight matrices descrambled for smooth propagation of data choose to propagate that data in a sinusoidal basis. Here this choice of X corresponds to the noise track taken in many signal processing applications. In particular if the SNR α^{-1} “equals” zero then the smoothness descramblers \widehat{P}_N tend to $T_r U_1^\top$. This limit produces a scaling law $P \rightarrow T_r^P \top U$. Under this scaling law, the minimizers $\widehat{P}(N) = T_r U_1^\top$ are scaled to I as $N \rightarrow \infty$. This scaling law will be used to justify the use of Fourier domain visualizations in [1]. We provide a more general version of the theorem in the Supplementary Information; here the choice of D as a finite difference stencil was taken to align the result with the experimental setup used in [1]

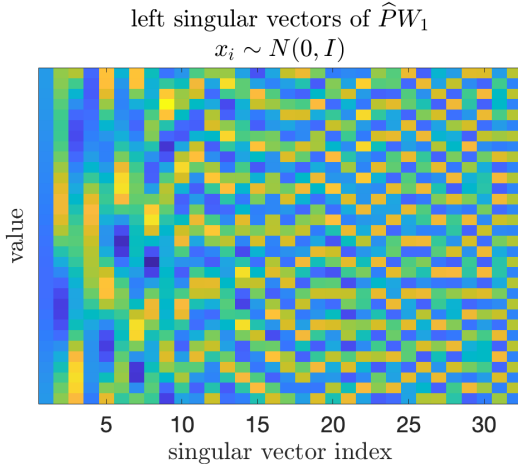


FIGURE 1. We sampled X in Equation 5 from a standard Gaussian ensemble and computed the left singular vectors of the first layer pre- and post-descrambling of the network in [30]. Note that the left singular vectors of the descrambled weight matrix are perfectly oscillating: this is because X as a standard Gaussian ensemble together with a linear wiretapped layer yields a descrambler $\widehat{P}(N) \approx T_r U^\top$, which results in $\widehat{P}W \approx T_r \Sigma V^\top$ so that the left singular vectors of the descrambled weight matrix are given by T_r .

In more realistic applied settings, training data is usually a mixture of signal and noise; we extend Theorem 1 to this case below. We recall that $k = 1$, so it will be dropped from the notation for clarity.

Linear Network, Noise and Signal. We consider the case when each training sample is $x = s(z) + \alpha^{-1}y$. First we observe that given an unbiased noise we have

$$(8) \quad \eta(P) \rightarrow \mathbb{E}[\|DPW(s(z))\|_2^2] + \alpha^{-2}\mathbb{E}[\|DPWy\|_2^2].$$

as $N \rightarrow \infty$ (see [SI appendix](#)). Thus, the objective function η splits into the sum of the *signal term* $\mathbb{E}[\|DPW(s(z))\|_2^2]$ and a noise term $\mathbb{E}[\|DPWy\|_2^2]$ weighted by the SNR α . Using (8) we show the following result for a noisy signal model.

Theorem 2. Borrowing notation from Theorem 1, let X be a $d \times N$ matrix of training data where each column is sampled from $x = s(z) + \alpha^{-1}y$. Denote $\widehat{P}(\alpha) := \lim_{N \rightarrow \infty} \widehat{P}(N)$ and let $\widehat{\mathcal{U}}(\alpha)$ be the matrix of left singular vectors of the descrambled weight matrix $\widehat{P}(\alpha)W$. Then $\mathcal{U}(\alpha)$ is continuous in α and as $\alpha \rightarrow 0$

$$(9) \quad \|\widehat{\mathcal{U}}(\alpha) - T_r\|_F \rightarrow 0.$$

Theorem 2 shows that the left singular vector basis of the descrambled matrix are “close” to a trigonometric basis, and extent of this proximity is controlled by the signal to noise ratio α^{-1} . As $\alpha \rightarrow 0$ this basis converges to the trigonometric basis (which is consistent with the case of Theorem 1).

Non-linear network. Finally, we proceed to discuss the non-linear case when $k \geq 2$. In this situation we choose to deal with the non-linearities using the Taylor expansion at the sample mean \overline{X} :

$$(10) \quad \widehat{P}(k, N) \approx \underset{P^\top P}{\operatorname{argmin}} \mathbb{E}[\|DP(f_k(\overline{x}) + Jf(\overline{x})^\top(X - \overline{x}))\|_2^2]$$

Now the RHS can be characterized through Theorems 1 and 2 applied to $Jf(\overline{X})$. We were able to also provide empirical evidence for the quality of the Jacobian approximation to the descrambling problem in Figure 2.

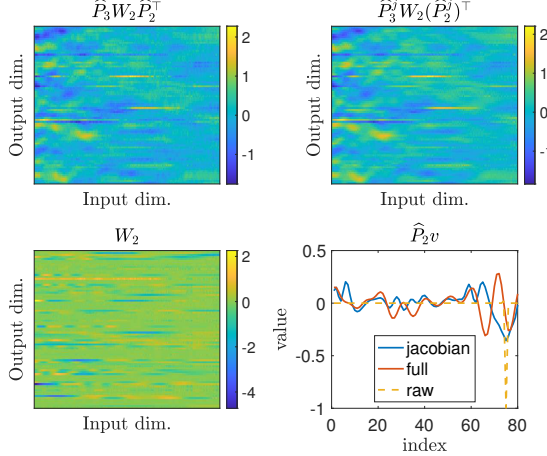


FIGURE 2. We compare the descramblers computed for $k = 2$ in DEERnet with $f_2(X)$ (termed full) and with the approximation in (10) (termed jacobian). We find that the overall descrambled matrices are visually similar (albeit not very interpretable). We also see, via the action of \widehat{P} on a singular vector, that the Jacobian descramblers \widehat{P}^j are an intermediate between full descrambling and no descrambling (bottom right).

3. APPLICATIONS

Interpretable neural networks. We use the results from the preceding discussion to study two cases in which descrambling reveals information already available to us through some other well-understood transformation of the weights. The first example comes from convolutional neural networks (CNN’s).

Corollary 1. Adopting the assumptions of Theorem 1 with samples of noise X and $k = 1$, let f be a 1-D CNN with stride 1. Then $\widehat{P}(k)W = W$, i.e., descrambling acts as identity transformation on the weight matrix.

Corollary 1 presents a simple case where descrambling becomes ineffective. This sheds light onto the limitations of this method when it comes to network interpretation. More pertinently, however, it shows that every choice of η , G , and X from (3) defines a class of k -interpretable weights \mathcal{I}_k such that the minimizers $\widehat{P}(\eta, G, k, N)$ converge to I whenever $W_k \in \mathcal{I}_k$ in the large data limit (here we change notation slightly

from (3) to include the effect of group G and criterion η). We formalize this intuition by defining a class of *interpretable* neural networks. In what follows we assume that \mathcal{N} is the set of fully connected neural networks.

Definition 2. An interpretability class $\mathcal{I}(\eta, G, k, x \sim \mu) \subset \mathcal{N}$ is the set of neural networks such that $f \in \mathcal{I}(\eta, G, k, x \sim \mu)$ if, for the k th layer, a group G , criterion η , and data X the solution to (3) where X has N i.i.d columns sampled by μ is $\widehat{P}(\eta, G, k, x \sim \mu) = I$ as $N \rightarrow \infty$. If $f \in \mathcal{I}(\eta, G, k, x)$ then f is said to be $\mathcal{I}(\eta, G, k, x)$ -interpretable, or simply \mathcal{I} interpretable if η, G, k and x are clear from context.

Interpretability classes quantify those neural networks which are interpretable after training and do not require any descrambling to be intelligible to humans/experts. In describing such neural networks, \mathcal{I} -classes account for the underlying problem (such as signal recovery/image classification) by tracking the distribution on the training data. Furthermore, definition 2 models a simple but natural setting used for training various types of neural networks: the training inputs are an incoming stream of samples of x forming the matrix of samples X . Under this training data regime, \mathcal{I} -interpretability record the large-data behaviour of the descrambling matrix \widehat{P} for a specific choice of wiretapped layer and descrambling criterion. *A priori* interpretability classes have a rather complicated structure and it is a mathematically interesting problem to provide some better understanding of different cases. In fact, we can reformulate Corollary 1 to give an explicit presentation for $\mathcal{I}(\eta, O(n), 1, x \sim N(0, \alpha^{-1}I))$ as the class of $1 - D$ neural networks which are convolutional in the first layer.

Proposition. Let $k = 1$, $G = O(n)$, η be the smoothness criterion descrambling functional ((5)) and let $x \sim \alpha^{-1}N(0, I)$ - the multivariate zero-mean normal distribution with variance $\alpha^{-2}I$. Let $\mathcal{C}_1^n \subset \mathcal{N}$ with a convolutional first layer with n nodes in the first hidden layer and let \mathcal{N} be the class of $1 - D$ NNs in $C(\mathbb{R}^n)^m$. Then, we have

$$(11) \quad \mathcal{I}(\eta, O(n), 1, (x, N(0, \alpha^{-1}I))) = \mathcal{C}_1^n.$$

As such, characterizing $\mathcal{I}(\eta, O(n), 1, (x, N(0, \alpha^{-1}I)))$ can seem unrealistic because most real-life instances of neural network training do not utilize purely noisy data. Recalling the context of inverse problems, it is of interest to know whether we can characterize any interpretability class when the input data is in the form of noisy measurements of a parameter. It turns out, for instance, that a simple phase identification problem in oscillatory data analysis (ODA) can be the right setting for such a question. A central problem in ODA is to identify the phases $\phi(t)$ and the trend $T(t)$ from the measurements of the noisy signal

$$(12) \quad f(t) = \exp 2\pi i \phi(t) + T(t) + y.$$

The signal model in (12) is ubiquitous in many applications of science and engineering, including clinical, seismic, and climate data, and investigative art [31, 32, 33, 34, 35, 36, 37, 38]. Unsurprisingly, this type of inverse problem has attracted neural network approaches [39]. Here we show that the simple case when the trend $T = 0$ and the phase $\phi = z$, a constant to be estimated under a uniform prior, the oscillatory data modeled by (12) defines a setting where we can characterize an interpretability class.

Corollary 2. Let $z \sim \text{Unif}[-uN, vN]$ be the phase parameter with uniform prior for $u, v \in \mathbb{Z}$ and the oscillating signal $s(z) = (\exp 2\pi i kT/N)_{k=0}^{N-1}$ be measured as $x = s(z) + \alpha^{-1}y$ where y is a standard normal variable. If η is the smoothness descrambling criterion then

$$(13) \quad \mathcal{I}(\eta, O(n), 1, x) = \mathcal{C}_1^n.$$

Here \mathcal{C}_1^n is the class of neural networks with a convolutional first layer and n nodes in the first hidden layer.

Corollary 2 has multiple implications. For example, it shows that convolutional neural networks reside in the class of interpretable networks for the problem of recovering the phase from equispaced samples of an oscillating signal in time. Second, it shows that descrambling the first layer for a network trained to solve this inverse problem might be inconclusive in yielding interpretations, because the descrambler transformation converges to the identity matrix. Thus, using smoothness descrambling for network interpretation reveals to us only the information already available in the raw weights of the first layer.

DEERNet. We use our theoretical analysis to furnish quantitative justifications for the visual descrambling analysis of DEERNet [1], the neural network on which descrambling was first tested. This theoretical perspective will illuminate why the SVD emerges as an “interpretable” factorization. DEERNet is a feedforward neural net trained to solve a noisy signal recovery problem in deep electron-electron resonance spectroscopy. In particular, it solves the following Fredholm equation of the first kind:

$$(14) \quad \Gamma(t) = \int_{\Omega} p(r) \gamma(r, t) dr + \xi.$$

Here $\gamma(r, t)$ is the DEER kernel given by

$$(15) \quad \gamma(r, t) := \sqrt{\frac{\pi r^3}{6Dt}} \left[\cos[Dt] C \left[\sqrt{\frac{6Dt}{\pi}} \right] + \sin[Dt] S \left[\sqrt{\frac{6Dt}{\pi}} \right] \right]$$

$$(16) \quad D := \frac{\mu_0 \gamma_1 \gamma_2 h}{4\pi r^3}; \quad FrC(x) = \int_0^x \cos(t^2) dt; \quad FrS(x) = \int_0^x \sin(t^2) dt.$$

The training inputs and outputs are of the form $\{d_i, p_i\}_{i=1}^N$, where p_i are distributions and Γ_i is the distance detected at times $\{t_j\}_{j=1}^{256}$, with Gaussian noise. DEERNet obtains p_i from d_i and hence can be formulated as a network that solves problem of recovering z from noisy observations of $x = s(z) + \alpha^{-1}y$. Here s represents the integral operator corresponding to integration against the DEER kernel and z is the input probability distribution.

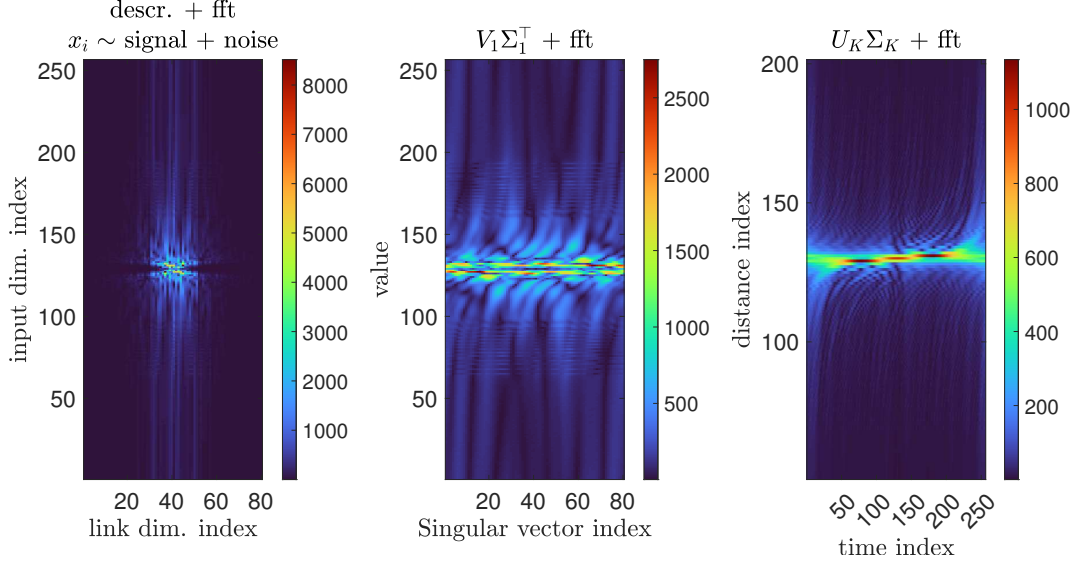


FIGURE 3. Left: Descrambling the first layer of a two-layer DEERNet reveals a notch and bandpass filter. A powerful plausibility argument is mounted in [1] to indicate that this notch resembles a cube root on the time axis/input dimension. Center: Visualize the Fourier transform of $\Sigma_1 V_1^\top$ (right) handily reveals repeating streaks along the singular vectors; in fact along the time axis we see these streaks arranged in the shape of a cubic. Right: We visualize the Fourier transform of the right singular vectors of the integral kernel K scaled by the singular values Σ_K and observe cubic streaks similar to the central panel. This provides a more quantitative justification for the first layer’s function as inverting the integral operator.

Why Fourier domain visualization works. In [1] a descrambling analysis of the first layer weights of a shallow 2-layer DEERnet uncovered a notch filter and a bandpass filter in the first weight matrix after visualizing the 2-D DFT $\mathcal{F}\hat{P}(1, N)W_1$ (Figure 3). Fourier domain visualization in [1] was justified experimentally because of the interlocking wave patterns seen in the descrambled weights $\hat{P}(1, N)W_1$. We now provide a more quantitative justification for this heuristic based on Theorem 1, and on the correspondence between

the SNR α^{-1} and the interpretation matrix $\widehat{P}(1, N)$. When the descrambling data X is purely noisy, $\widehat{P}(N) \rightarrow T_r U_1^\top \iff T_r^\top \widehat{P}(N) U_1 \rightarrow I$ due to Theorem 1. Thus, the group homomorphism

$$(17) \quad P \rightarrow \varphi(P) = T_r^\top P U_1$$

provides an appropriate rescaling for the limiting descrambling matrix $\widehat{P}(1)$. For example, when $\alpha^{-1} \rightarrow 0$, $\varphi(\widehat{P}(N)) \rightarrow I$, so that the group homomorphism (17) simplifies the correspondence between the SNR and the rescaled large-limit descrambler $\varphi(\widehat{P}(N))$. In this case specifically we have

$$(18) \quad \text{SNR} = 0 \iff \varphi(\widehat{P}) = I.$$

As a consequence, post-descrambling visualization of the 2D DFT of W_1 approximates $\varphi(\widehat{P}) \Sigma_1(\mathcal{F}V_1)^\top$. In fact, in the case when $\varphi(\widehat{P}) = I$, $\mathcal{F}\widehat{P}_1 W_1 \approx \Sigma_1(\mathcal{F}V_1)^\top$ - the Fourier transform of the singular vectors rescaled by the singular values. Thus, visualizing the matrix by setting $\varphi(P) = I$ is quite informative: the result is $\Sigma_1 V_1^\top$ and it reveals a repeating pattern of cubic streaks, uncovering both the notch filter and the distance cube root as found in the integral kernel from (14). This shows that descrambling uncovers - to a large extent - the information within the SVD and that multiplication by \widehat{P}_1 moves W_1 closer to the integral kernel. Singular vectors themselves can be interpretable without necessitating any additional processing such as descrambling, intertwiner groups, or hypergraph arrangements [13, 12] in the context of noisy signal estimation.

Connection to semantic development. The emergence of the DEER kernel in the right singular vector matrix V_1 is not entirely surprising due to a heuristic motivated by (1). Indeed, if the network did not have a non-linearity, then $W_1(t) = Q^{-1}A(\Lambda, t)V^\top$ where V is the matrix of the right singular vectors of $\Sigma_{yx} = \mathbb{E}[yx^\top]$, the output-input covariance matrix. But in the signal estimation case where $y = s(x) + \alpha^{-1}\xi$, this covariance matrix has a very simple form, especially when s is a linear map. In this case, we have $\Sigma_{yx} = \mathbb{E}_{yx}[Kxx^\top K^\top] = K\mathbb{E}[xx^\top]K^\top$. With the assumption that $\mathbb{E}[xx^\top] = I$, we have $\Sigma_{yx} = KK^\top$ so the matrix V corresponds to the spectral decomposition of the kernel KK^\top . We confirm this heuristic in the right panel of Figure 3

Noise isn't always meaningless. Our analysis of DEERnet shows that descrambling goes hand-in-hand with semantic development in the SVD, particularly when a network is trained to learn a signal from noisy measurements. However, this interplay with semantic development is only approximate. This is because the linear network training dynamics (1) merely approximates the real training dynamics of nonlinear networks. This necessitates the discovery of nonlinear features via descrambling. For example, the notch filter in the first layer of DEERnet cannot be discovered by noise-only descrambling, and we require the presence of the forward map s in the propagating data to discover a notch that is latent in W_1 .

Here we describe a case where noise descrambling, i.e the neural network interpretation via its singular vectors, is useful in and of itself. We demonstrate this phenomenon for a NN in which the forward map s is non-linear, so that the nature of matrices U and V in (1) is entirely unspecified. In particular, following [30] we train a four layer fully-connected NN to learn the exponential parameters $(T_{2,1}, T_{2,2})$ generating a biexponential model:

$$(19) \quad y(t) = 0.6 \exp(-t/T_{2,1}) + 0.4 \exp(-t/T_{2,2},)$$

corrupted by noise. The recovery of exponential parameters $T_{2,1}, T_{2,2}$ from a noisy decay curve is a central problem in magnetic resonance relaxometry [40], and is well-known to be ill-posed with parameter estimates strongly dependent on the noise. This problem has been investigated with a number of neural network-based approaches [41, 42]; the novelty of the network in [30] is that it is trained to solve this problem on both noisy and smooth forms of the same data, as a form of input data transformation to incorporate high-fidelity and high-stability and generalizability characteristics into the solutions. To achieve this, the noisy input data is first processed with regularized non-linear least squares parameter estimation, with these estimates used to generate smooth decay curves. These smooth curves are concatenated with the noisy samples to form a single input sample for presentation to the NN. The NN with just the native input, concatenated with itself, is termed (ND, ND), where ND indicates noisy decay. The NN with the concatenated native and smoothed versions of the decay curve is termed (ND, Reg), with Reg indicating the smooth decay generated by the regularized nonlinear least squares analysis. This strategy of training on both noisy and smooth data is termed *input layer regularization*, and improves parameter estimation by 5-10 percent as compared to

the more conventional NN estimation of parameters from noisy decay curves [30]. We find that the right singular vectors corresponding to the largest singular values of the first layer are biexponential curves, so that the network learns an input signal library in the class of its training data. Most notably, the (ND, Reg) network learns two very different shapes of biexponential for the noisy and smooth case; we attribute its higher test accuracy as compared to (ND, ND) to this result, indicating that (ND, Reg) learns a larger set of functions within the signal model class of biexponential functions. Thus, in the regression setting the descrambling guides us to finding the location of NN learning, namely within the SVD. In addition to explaining generalization, learning of the model in the SVD may have adversarial implications since we are able to learn samples of the input data model directly from a trained network. While the SVD has been used as a compression technique in feedforward neural networks [23] and deep layer interpretation in classification [11, 13], our results appear to be the first demonstration that data model learning occurs in singular vectors for nonlinear networks.

4. CONCLUSION

A key novelty of descrambling is that it leverages problem-dependent interpretation, akin to the manner in which interpretability methods in image classification concern the most influential pixels, image substructures, and, decision boundaries. We take this concept further: our characterization of solutions to (5) and the subsequent theoretical explanations to the experimental results in [1] show that the interpretation matrices \hat{P} can admit simple large-data limits that depend on the underlying problem. In fact, we observe that the mathematical formalism in inverse problems allows us to obtain strong characterizations of these limits with practical implications. For example, descrambling implicitly defines problem-dependent classes of neural networks - and these classes can be explicitly characterized, for instance, in a simple problem from oscillatory data analysis. Furthermore, while [1] interprets DEERNet through the SVD of the descrambled weights, we show that even the SVDs of the *scrambled*, i.e., raw, weights can themselves be informative. We give an explanation for this phenomenon - if the data is highly noisy, the Fourier domain visualization of the

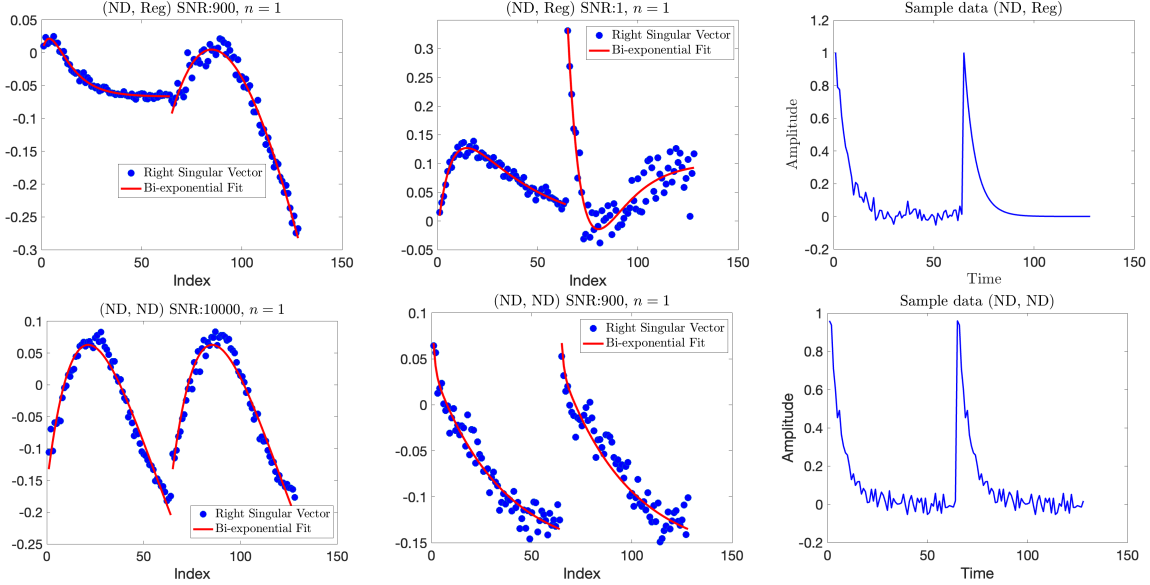


FIGURE 4. We visualize the singular vectors of the first layer of ILR networks trained on concatenations of noisy time-series data with the functional form $c_1 \exp(-t/T_{2,1}) + c_2 \exp(-t/T_{2,2})$ for $c_i \geq 0$, discovering that these singular vectors themselves can be fit by curves of the same algebraic form as the noise-less version of the training data, allowing for the c_i 's to be negative. Note that this phenomenon persists for a variety of SNR's and for both classes of networks—(ND, ND) and (ND, Reg). Here (ND, Reg) refers to networks trained on data points given by a concatenation of noisy and Tikhonov regularized copies of the same data (right panel).

descrambled weights approximates the Fourier domain visualization of the orthogonal row basis vectors provided by the right singular vectors through the rescaling formula motivated by Theorem 1. We remark, however, that this does not imply that descrambling is equivalent to the SVD -indeed, in the cases when the data X follows the more realistic distribution of a signal under noisy measurements and the network is wiretapped at a higher layer ($k \geq 2$) we can no longer exactly characterize the solutions to (5) and the minimizers do indeed reflect the latent transformations in the underlying weights W_k . We find, at least empirically that the action of descrambler matrices can be approximated through descrambling of the network linearized its Jacobian at the empirical average. This does not mean the choice of the Jacobian as a linear approximation is canonical--there are many different linear models for NN's [43, 44, 45] and it is yet unclear which approximation serves best as a surrogate for modeling the action of descrambling transformations.

A surprising and highly significant aspect of our results is that when the SVD is uncovered indirectly by descrambling, it *still* remains informative of the transformations in the data. This observation closely resembles examples [13, 12, 46] where SVDs of weights in CNNs are used to interpret features of an image classification network. Unlike these approaches - which require highly non-trivial post-processing of the singular vectors - we demonstrate that a simple visual analysis of singular vectors themselves can inform the post hoc analysis of the network's performance. Moreover we show that in noisy estimation problems it is the SVD where the network memorizes the underlying function class of the problem. This demonstrates not only that the training dynamics given by (1) for linear models can approximate non-linear settings but more also that the SVD by itself can illuminate the network's generalizability and interpretability.

MATERIALS AND METHODS

The proofs all our results and supporting figures have been provided in the SI document. Code for the figures and additional experiments can be found at <https://github.com/ShashankSule/descrambling-NN>

ACKNOWLEDGEMENTS

This work was supported in part by the Intramural Research Program of the National Institute on Aging of the National Institutes of Health (NIH).

APPENDIX
THEORETICAL RESULTS

Here we provide proofs for the results in our submitted article.

Lemma 1. Let W_n be a sequence of matrices such that $W_n \rightarrow W$ in the Frobenius norm where $W \in A$, where A is the set of matrices with distinct non-zero singular values. Then the (right and left) singular vectors $\{u_i^n\}$ and $\{v_i^n\}$ of W_n converge to the right (resp. left) singular vectors of W .

Proof. Since u_i^n and v_i^n are the eigenvectors of WW^\top and $W^\top W$ respectively, we drop without losing generality to the case where W is symmetric, so it has real eigenvalues. But from [29, Theorem 8, pp. 130], the eigenvectors of a matrix with simple eigenvalues are differentiable in its entries. Consequently, if u_i^n is the i th eigenvector of W_n then $u_i^n \rightarrow u_i$ where u_i is the i th eigenvector of W . \square

Theorem 1. For the reader's convenience we repeat the statement of the theorem here. Let

- (1) D be a Fourier/finite difference stencil [47]
- (2) X_N a random $d \times N$ matrix such that each column x_i is drawn independently from an isotropic density.
- (3) W any $m \times d$ weight matrix with ordered rank r SVD $W = U\Sigma V^\top$
- (4) T the $m \times m$ matrix such that every k th column has l th entry $t_k(l)$ given by

$$(20) \quad t_k(l) = \begin{cases} \cos \frac{\pi lk}{m} & k \text{ even} \\ \sin \frac{\pi l(k+1)}{m} & k \text{ odd} \end{cases}$$

- (5) T_r the submatrix of T given by picking the last r columns.

Then we have that

$$\hat{P}_N = \operatorname{argmin} \|DPWX_N\|_F^2 \text{ w.r.t } P^\top P = I \longrightarrow T_r U^\top$$

almost surely as $N \rightarrow \infty$. In particular the descrambled weight matrix converges to $T_r \Sigma V^\top$ almost surely.

Proof. First to clean up some notation we set $S_N := WX_N$. Now note that

$$\operatorname{argmin}_{P^\top P = I} \|DPWX\|_F^2 = \operatorname{argmin}_{P^\top P = I} \frac{1}{N} \|DPWX\|_F^2$$

So we can switch to analyzing the minimum of $\frac{1}{N} \|DPWX\|_F^2$. But now,

$$(21) \quad \frac{1}{N} \|DPWX_N\|_F^2 = \frac{1}{N} \operatorname{Tr}(DPWX(DPWX)^\top)$$

$$(22) \quad = \frac{1}{N} \operatorname{Tr}(DPWXX^\top W^\top P^\top D^\top)$$

$$(23) \quad = \operatorname{Tr}\left(DPW\left(\frac{1}{N}X_N X_N^\top\right) W^\top P^\top D^\top\right)$$

$$(24) \quad = \operatorname{Tr}(DPS_N S_N^\top P^\top D^\top)$$

$$(25) \quad = \operatorname{Tr}(S_N^\top P^\top D^\top DPS_N)$$

To find the minimizer to (25) w.r.t $P^\top P = I$ we make an interesting change of variable: let $S_N = U_N \Sigma_N V_N$ be the SVD of $S_N := W\left(\frac{1}{N}X_N X_N^\top\right)W^\top$. Then we let $Y_N = PS_N V_N$. Note that this means $Y_N^\top Y = \Sigma_N^2$ given the constraint $P^\top P$. With this change of variables (25) can be written as

$$(26) \quad \frac{1}{N} \|DPWX_N\|_F^2 = \operatorname{Tr}(Y^\top D^\top DY)$$

Consequently, the smoothness descrambling problem

$$(27) \quad \min \|DPWX_N\|_F^2 \quad \text{w.r.t } P^\top P = I$$

can be relaxed to

$$(28) \quad \min \operatorname{Tr}(Y^\top D^\top DY) \quad \text{w.r.t } Y^\top Y = \Sigma_N^2.$$

Note that the optimization problem 27 is a relaxation of 28 because of the transformation $P \rightarrow PWV$. But now the solution to the relaxed problem 28 is well-known: it is a generalized eigenvalue problem whose solutions correspond to the first $R_N = \min(r_N, d-1)$ eigenvectors of $D^\top D$ where r_N is the number of non-zero diagonal entries in Σ_N^2 (this is because notably any finite difference stencil has rank $d-1$). Since $D^\top D$ is diagonalized by T , we pick the largest R_N eigenvectors (indexed by the matrix T_{R_N}) and scale them by Σ_N to get Y . Thus, $Y = T_{R_N} \Sigma_{R_N}$. Now using the change of variables $Y = PS_N V_{R_N}$ we get $PS_N = T_{R_N} \Sigma_{R_N} V_{R_N}^\top$ so $S_N = P^\top T_{R_N} \Sigma_{R_N} V_{R_N}^\top$. This is a singular value decomposition for S_N , so as long as the non-zero singular values of S_N are distinct we get from the uniqueness of the SVD that $\widehat{P}_N^\top T_{R_N} = U_N \iff \widehat{P}_N = T_{R_N}(U_N)_{R_N}$. Now this is where the assumption that $W \in A$ comes in: due to the strong law of large numbers we have that $S_N \rightarrow WW^\top$ almost surely. Since the singular values of W are distinct and we get that the singular values of S_N are eventually distinct and ordered according to the ordered of W so the expression for \widehat{P}_N is valid; moreover from Lemma 1 we get that the matrices $(U_N)_{R_N}$ will converge to the left singular vectors of U of W . This proves our result. \square

Equation [10]. Let $x = s(z) + \alpha^{-1}y$ where y is a zero-mean isotropic noise vector with finite second moment and z has some prior distribution independent of the noise y . We stated the following convergence result:

$$(29) \quad \eta(P) \rightarrow \mathbb{E}[\|DPW(s(z))\|_2^2] + \alpha^{-2}\mathbb{E}[\|DPW y\|_2^2]$$

The proof of (8) is as follows: Note first that because of the law of large numbers,

$$\frac{1}{N}\|DPWX\|_F^2 = \frac{1}{N}\sum_{i=1}^N\|DPWx_i\|_2^2 \rightarrow \mathbb{E}_{z,y}[\|DPWx\|]$$

We directly switch to analyzing the LLN limit of η and write

$$\eta(P) = \mathbb{E}[\|DPWx\|_2^2] = \mathbb{E}[\mathbb{E}[\|DPWx\|_2^2 | z]] = \mathbb{E}[\mathbb{E}[\|DPW(s(z) + \alpha^{-1}y)\|_2^2 | z]]$$

Now setting $A = DPW$ and using the zero-mean property of the additive noise we get

$$(30) \quad \begin{aligned} \eta(P) &= \mathbb{E}\left[\mathbb{E}[\|A(s(z))\|_2^2 | z] + \mathbb{E}[\|A(\alpha^{-1}y)\|_2^2 | z]\right. \\ &\quad \left.+ 2\alpha^{-1}\mathbb{E}[\langle A^\top A(s(z)), y \rangle | z]\right] \\ &= \mathbb{E}\left[\mathbb{E}[\|A(s(z))\|_2^2 | z] + \mathbb{E}[\|A(\alpha^{-1}y)\|_2^2 | z]\right] \\ &= \mathbb{E}[\|A(s(z))\|_2^2] + \alpha^{-2}\mathbb{E}[\|Ay\|_2^2] \\ &= \mathbb{E}[\|DPW(s(z))\|_2^2] + \alpha^{-2}\mathbb{E}[\|DPW y\|_2^2] \end{aligned}$$

Now we state Theorem 2:

Theorem 2. Borrowing notation from Theorem 1, let X be a $d \times N$ matrix of training data where each column is sampled from $x = s(z) + \alpha^{-1}y$. Denote $\widehat{P}(\alpha) := \lim_{N \rightarrow \infty} \widehat{P}(N)$ and let $\widehat{U}(\alpha)$ be the matrix of left singular vectors of the descrambled weight matrix $\widehat{P}(\alpha)W$. Then $\widehat{U}(\alpha)$ is continuous in α and as $\alpha \rightarrow 0$

$$(31) \quad \|\widehat{U}(\alpha) - T_r\|_F \rightarrow 0.$$

Proof. We can use the same analysis as the proof of Theorem 4 to conclude first that $\widehat{P}_N = T_{R_N}(U_N)_{R_N}$; here U_N is the matrix of left singular vectors of $W\frac{1}{N}(X_N X_N^\top)W^\top$. Then $(X_N X_N^\top) \rightarrow \mathbb{E}_X[xx^\top]$, the autocorrelation matrix of X . But as $\alpha \rightarrow 0$, this autocorrelation matrix converges to I . Once again using the continuity of eigenvectors in the entries of the matrix, we get that $U(\alpha) \rightarrow U$, where $U(\alpha)$ is the matrix of singular vectors of $W\mathbb{E}[xx^\top]W^\top$ and U is the matrix of singular vectors of W . \square

Finally, we state and prove Corollary 1 and 2 pertaining to convolutional neural networks and oscillatory data analysis:

Corollary 1. Adopting the assumptions of Theorem 1 with samples of noise X and $k = 1$, let f be a 1-D CNN with stride 1. Then $\widehat{\mathcal{P}}(k)W = W$, i.e., descrambling acts as identity transformation on the weight matrix.

Proof. If f is a 1-D CNN where the first filter W has stride 1 then W is symmetric and circulant so $W = T\Sigma T^\top$ where T is the matrix of samples of a trigonometric basis from Theorem 1. Then $P = T_r^\top T_r = I_r$. \square

Corollary 2. Adopting the assumptions of Theorem 1, let $z \sim \text{Unif}[-uN, vN]$ for $u, v \in \mathbb{Z}$ and $s(z) = (\exp 2\pi i k T/N)_{k=0}^{N-1}$. Then $\widehat{\mathcal{P}}(N) \rightarrow \widehat{\mathcal{P}} = T_r U^\top$ where T_r is the trigonometric basis from Theorem 1 and U is the left singular vector matrix of the weights W .

Proof. We show that the signal term and noise term reduce to the same minimization problem. Let $A := DPW$. Then we have

$$\mathbb{E}_z[DPWs(z)] = \mathbb{E}_z[As(z)] = \frac{1}{N(u+v)} \int_{-uN}^{vN} \|As(z)\|_2^2 dz$$

But now, $(As(z))_j \overline{(As(z))_j} = \sum_{k,l} a_{jk} a_{jl} \exp 2\pi i (k-l)z/N$, and

$$(1/N(u+v)) \int_{-uN}^{vN} \exp 2\pi i (k-l)z/N dz = \delta_{l,k}$$

Here $\delta_{k,l}$ is the Kronecker delta. Now,

$$\begin{aligned} \frac{1}{N(u+v)} \int_{-uN}^{vN} \|As(z)\|_2^2 dz &= \frac{1}{N(u+v)} \int_{-uN}^{vN} \sum_j (As(z))_j \overline{(As(z))_j} dz \\ &= \sum_j \frac{1}{N(u+v)} \int_{-uN}^{vN} (As(z))_j \overline{(As(z))_j} dz \\ &= \sum_j \sum_k |a_{j,k}|^2 \\ &= \|A\|_F^2 = \|DPW\|_2^2 \end{aligned}$$

Putting the above calculation together with the calculation for isotropic noise from Theorem 1 and using Equation (8) we get

$$\begin{aligned} \eta(P) &= \mathbb{E}_z[DPWs(z)] + \alpha^{-2} \mathbb{E}[\|DPW\|_2^2] \\ &= \|DPW\|_2^2 + \alpha^{-2} \|DPW\|_2^2 \end{aligned}$$

Minimizing the above function for P orthogonal leads to $P = T_r^\top U$ (just like Theorem 1). \square

MDS Criterion. The *maximum diagonal sum* (MDS) criterion is suggested in [1] for NN interpretation of frequency domain data:

$$\widehat{P}_{MDS} = \underset{P^\top P = I}{\text{argmax}} \text{Tr}(PW)$$

We show that for this criterion \widehat{P} can be given explicitly in terms of the SVD of weights W :

Proposition. Let $W \in M_n(\mathbb{R})$. Then $\underset{P^\top P = I}{\text{argmax}} \text{Tr}(PW) = VU^\top$ where $W = U\Sigma V^\top$ is the SVD of W .

Proof. Let $W = \sum_{i=1}^r \sigma_i u_i v_i^\top$ be the SVD of W and let P be orthogonal. Then

$$\text{Tr}(PW) = \sum_{i=1}^r \sigma_i \text{Tr}(Pu_i v_i^\top)$$

But note that $\text{Tr}(xy^\top) = \langle x, y \rangle$ so $\text{Tr}(Pu_i v_i^\top) = \langle Pu_i, v_i \rangle \leq \|Pu_i\|^2 \|v_i\|^2 = 1$ using Cauchy-Schwarz. So

$$Tr(PW) = \sum_{i=1}^r \sigma_i Tr(Pu_i v_i^\top) \leq \sum_{i=1}^r \sigma_i = Tr(\sqrt{W^\top W})$$

Thus $\hat{P} = VU^\top$ yields the conclusion. \square

DEERNet. We descrambled DEERNet according to the specifications in [1]. In particular we used the shallow architecture Input \rightarrow Fully connected $256 \times 80 \rightarrow$ tanh activation \rightarrow Fully connected $80 \times 256 \rightarrow$ sigmoid activation \rightarrow renormalization \rightarrow Output. Additionally, we made use of the MATLAB modules in the Spinach package to train the network and descramble it on a Quadro GV100 GPU to reproduce the experiments in [1] as closely as possible. We were able to reproduce these experiments only up to an amount of noise—the recovery of the cubic notch filter is much clearer in [1] and may have contributed to the interpretation of the first layer as notch filter/baseline elimination. Nonetheless, in our main article we have also given a quantitative explanation for why the first layer represents the DEER kernel based on a rescaling analysis motivated by Theorem 1. We also confirmed the existence of cubic conversion by changing the cubic factor in the DEER kernel to a quartic factor and finding a narrowing in the notch presumably to account for the fact that a quartic curve is flatter around the origin than a cubic. This experiment has been provided in our data repository <https://github.com/ShashankSule/descrambling-NN>.

ILR network. We trained neural networks with a $128 \rightarrow 32 \rightarrow 256 \rightarrow 256 \rightarrow 2$ input layer regularization structure with ReLU non-linearities to solve the problem of recovering $(T_{2,1}, T_{2,2})$ from 64 noisy time-equispaced measurements of the signal

$$(32) \quad 0.6 \exp(-t/T_{2,1}) + 0.4 \exp(-t/T_{2,2})$$

The raw noisy data track (termed ND) was processed through a non-linear least squares problem and the resulting NLLS-recovered parameters $(T_{2,1}^{NLLS}, T_{2,2}^{NLLS})$ were used to generate a new track (termed Reg) using equispaced time samples. The concatenated data, now of 128 measurements, was fed through the network with RMSE loss to recover the original $(T_{2,1}, T_{2,2})$. Following the recommendations in [30] we used a Tikhonov regularization procedure in the NLLS pre-processing step with $\lambda = 1.6 \times 10^{-4}$. We also trained the same architecture by concatenating the same sample of noisy data into a size 128 vector; this architecture is termed (ND,ND) and it represents the traditional neural-network approach of recovering parameters from noisy samples of a signal. Post-training we compute the singular vectors of the weight matrices W_1 , finding that these singular vectors themselves are noisy samples of biexponential curves. The caveat here, however, is that we required biexponential functions of the form $c_1 \exp(-t/T_{2,1}) + c_2 \exp(-t/T_{2,2})$ where $c_1, c_2, T_{2,1}, T_{2,2}$ could be any real number. As a consequence, these singular vector curves cannot necessarily fit a *decaying* biexponential model. We infer from this that the first layer seems to learn the general signal model rather than training examples themselves.

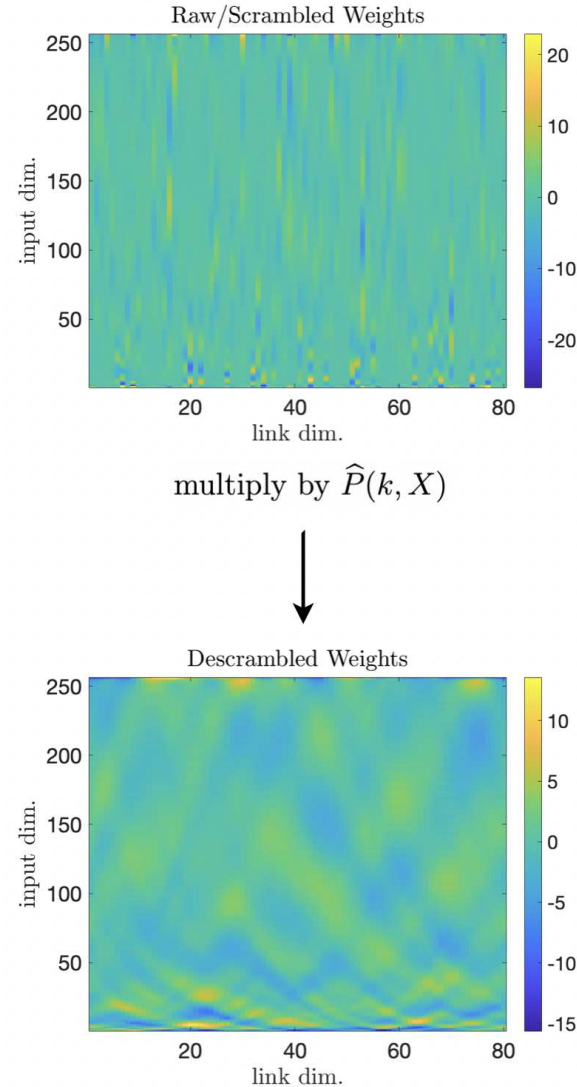


FIGURE 5. Descrambling the first layer of DEERNet reveals interlocking wave patterns, hinting at the transformation underlying this weight matrix

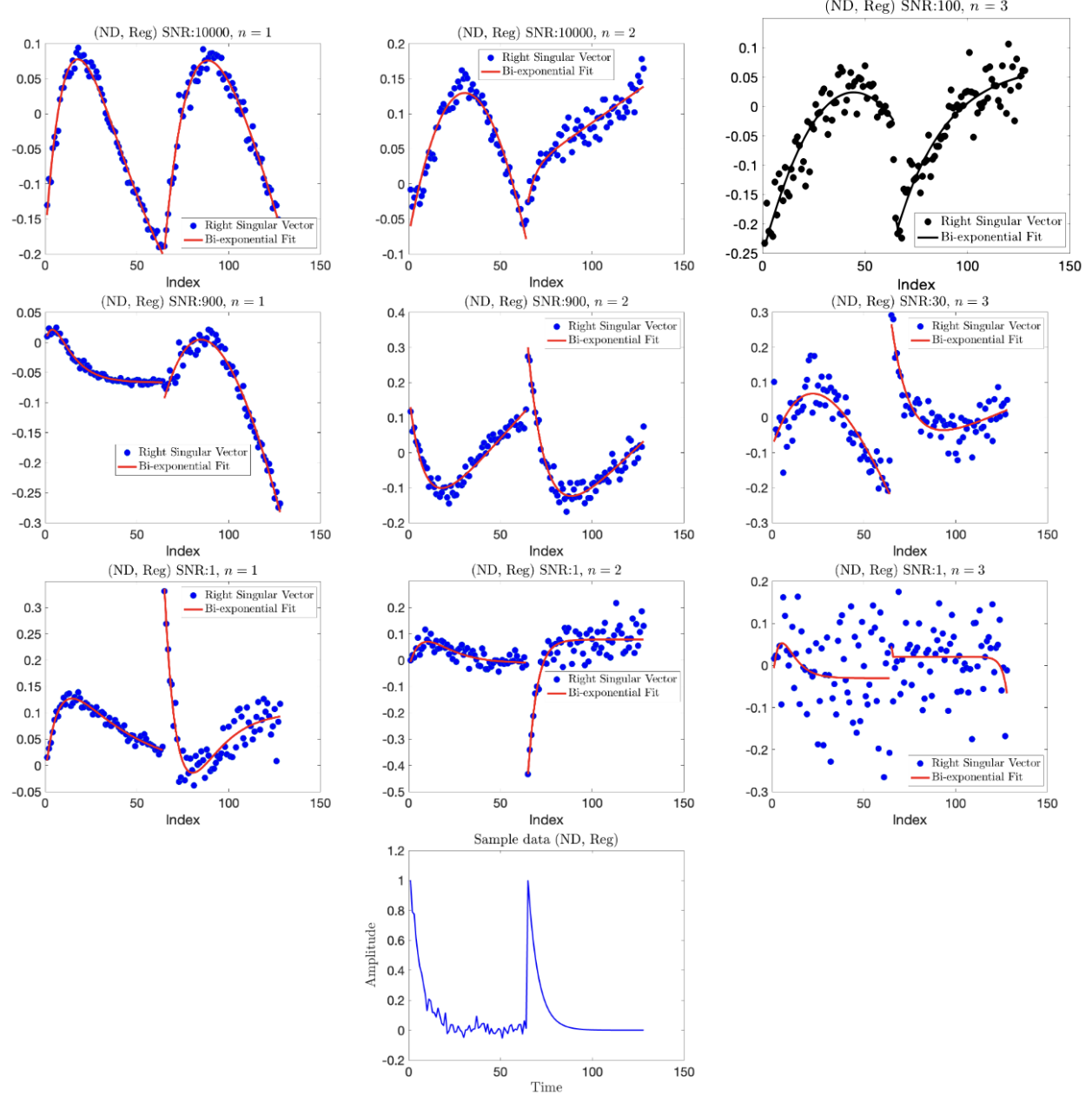


FIGURE 6. Visualizing the three right singular vectors corresponding to the largest singular values for the first weight matrix in (ND, Reg) networks for $\text{SNR} = 100, 30, 1$. We find that these vectors can be fit with a (not necessarily decaying) biexponential model. In fact the singular vectors themselves are split along the 64th entry (akin to the training data) with a different biexponential curve being learned for each half. The curves learned for the noisy half vs the smooth half are markedly different in shape, enabling us to better understand why (ND,Reg) generalizes better than (ND,ND)

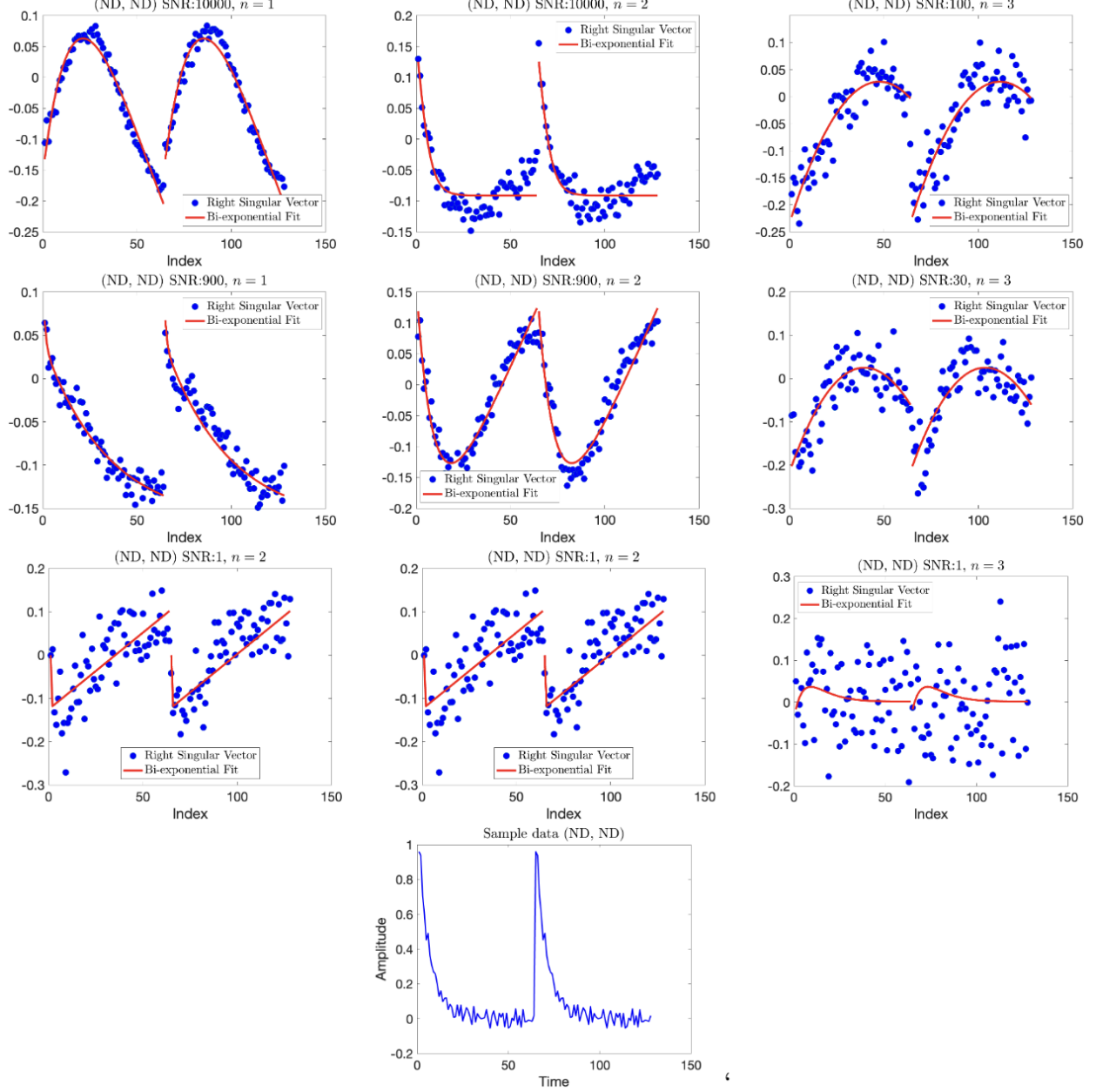


FIGURE 7. Visualizing the three right singular vectors corresponding to the largest singular values for the first weight matrix in (ND, ND) networks for $\text{SNR} = 100, 30, 1$. We witness a similar pattern to the (ND, Reg) networks where the singular vectors can be fit with a biexponential model, concluding that singular vector model learning is truly a consequence of the data and not the concatenation procedure. Clearly, since both halves of the data are the same, the singular vectors on both halves the data are also nearly identical. Thus the signal model library learned by the weights of the NN is less diverse, and may be responsible for the lower test accuracy of the NN

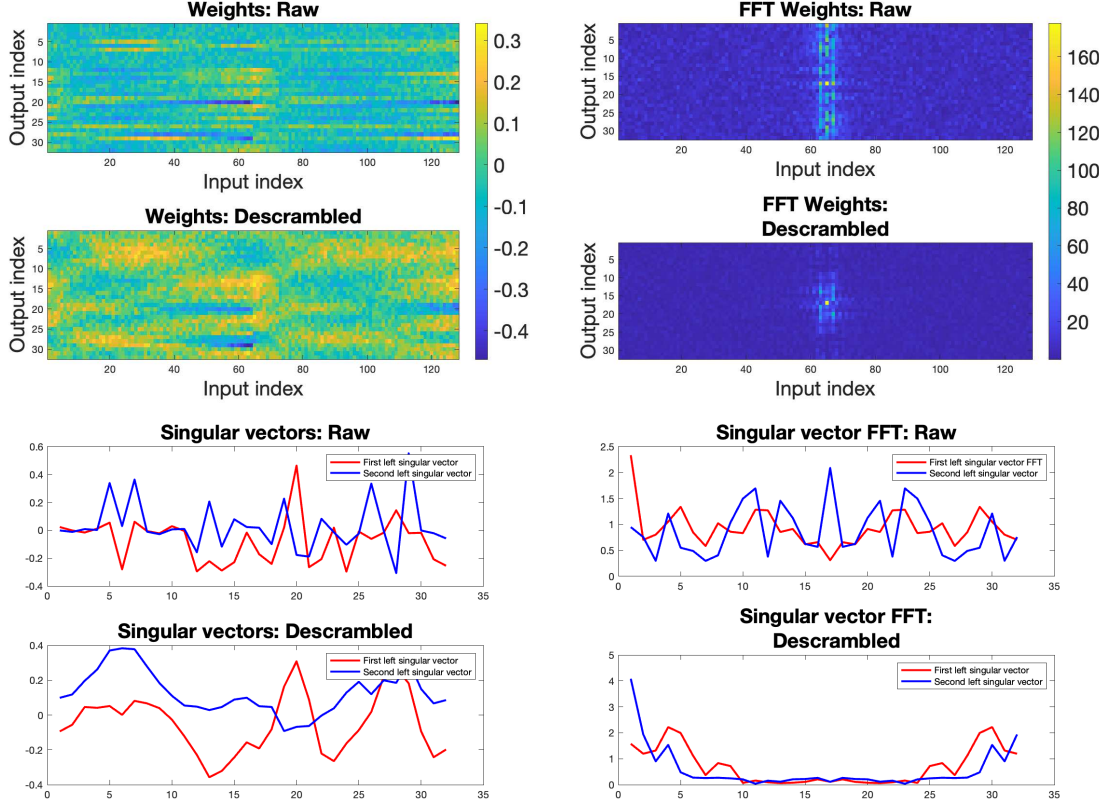


FIGURE 8. We also descrambled the first layer of an SNR 10, (ND, Reg) network with its input data. However, unlike what was done for DEERNet, we were not able to discern the underlying transformation of this layer from its Fourier signature, or from the descrambled singular vectors. In fact, after descrambling with data only from the noise track we found the descrambled matrices much more interpretable; Theorem 4 explained why—this was because we were actually visualizing the right singular vectors, which turn out to be samples of a biexponential model.

REFERENCES

- [1] Jake L Amey et al. “Neural network interpretation using descrambler groups”. In: *Proceedings of the National Academy of Sciences* 118.5 (2021).
- [2] Andrew M Saxe, James L McClelland, and Surya Ganguli. “A mathematical theory of semantic development in deep neural networks”. In: *Proceedings of the National Academy of Sciences* 116.23 (2019), pp. 11537–11546.
- [3] Erik Strumbelj and Igor Kononenko. “An efficient explanation of individual classifications using game theory”. In: *The Journal of Machine Learning Research* 11 (2010), pp. 1–18.
- [4] Feng Wang, Haijun Liu, and Jian Cheng. “Visualizing deep neural network by alternately image blurring and deblurring”. In: *Neural Networks* 97 (2018), pp. 162–172.
- [5] Aravindh Mahendran and Andrea Vedaldi. “Understanding deep image representations by inverting them”. In: *Proceedings of the IEEE conference on computer vision and pattern recognition*. 2015, pp. 5188–5196.
- [6] Anh Nguyen et al. “Synthesizing the preferred inputs for neurons in neural networks via deep generator networks”. In: *Advances in neural information processing systems* 29 (2016).
- [7] Fahim Dalvi et al. “What is one grain of sand in the desert? analyzing individual neurons in deep nlp models”. In: *Proceedings of the AAAI Conference on Artificial Intelligence*. Vol. 33. 01. 2019, pp. 6309–6317.
- [8] Dumitru Erhan et al. “Visualizing higher-layer features of a deep network”. In: *University of Montreal* 1341.3 (2009), p. 1.
- [9] Anh Nguyen et al. “Plug & play generative networks: Conditional iterative generation of images in latent space”. In: *Proceedings of the IEEE conference on computer vision and pattern recognition*. 2017, pp. 4467–4477.
- [10] Karen Simonyan, Andrea Vedaldi, and Andrew Zisserman. “Deep inside convolutional networks: Visualising image classification models and saliency maps”. In: *arXiv preprint arXiv:1312.6034* (2013).
- [11] Maithra Raghu et al. “Svcca: Singular vector canonical correlation analysis for deep learning dynamics and interpretability”. In: *Advances in neural information processing systems* 30 (2017).
- [12] Charles Godfrey et al. “On the Symmetries of Deep Learning Models and their Internal Representations”. In: *arXiv preprint arXiv:2205.14258* (2022).
- [13] Brenda Praggastis et al. “The SVD of Convolutional Weights: A CNN Interpretability Framework”. In: *arXiv preprint arXiv:2208.06894* (2022).
- [14] Sven Hammarling. “The singular value decomposition in multivariate statistics”. In: *ACM Signum Newsletter* 20.3 (1985), pp. 2–25.
- [15] Erkki Oja. “The nonlinear PCA learning rule in independent component analysis”. In: *Neurocomputing* 17.1 (1997), pp. 25–45.
- [16] Michael E Wall, Andreas Rechtsteiner, and Luis M Rocha. “Singular value decomposition and principal component analysis”. In: *A practical approach to microarray data analysis*. Springer, 2003, pp. 91–109.
- [17] Isaac J Schoenberg. “Metric spaces and positive definite functions”. In: *Transactions of the American Mathematical Society* 44.3 (1938), pp. 522–536.
- [18] Benyamin Ghojogh et al. “Multidimensional scaling, sammon mapping, and isomap: Tutorial and survey”. In: *arXiv preprint arXiv:2009.08136* (2020).
- [19] J Álvarez-Vizoso et al. “Geometry of curves in \mathbb{R}^n from the local singular value decomposition”. In: *Linear Algebra and its Applications* 571 (2019), pp. 180–202.
- [20] Robert T Arn et al. “Motion segmentation via generalized curvatures”. In: *IEEE transactions on pattern analysis and machine intelligence* 41.12 (2018), pp. 2919–2932.
- [21] Gao Daqi and Wu Shouyi. “An optimization method for the topological structures of feed-forward multi-layer neural networks”. In: *Pattern recognition* 31.9 (1998), pp. 1337–1342.
- [22] C-S Cheng. “A neural network approach for the analysis of control chart patterns”. In: *International Journal of Production Research* 35.3 (1997), pp. 667–697.
- [23] Huanrui Yang et al. “Learning low-rank deep neural networks via singular vector orthogonality regularization and singular value sparsification”. In: *Proceedings of the IEEE/CVF conference on computer vision and pattern recognition workshops*. 2020, pp. 678–679.

- [24] Shengze Cai et al. “Physics-informed neural networks (PINNs) for fluid mechanics: A review”. In: *Acta Mechanica Sinica* (2022), pp. 1–12.
- [25] Alice Lucas et al. “Using deep neural networks for inverse problems in imaging: beyond analytical methods”. In: *IEEE Signal Processing Magazine* 35.1 (2018), pp. 20–36.
- [26] Jonas Adler and Ozan Öktem. “Solving ill-posed inverse problems using iterative deep neural networks”. In: *Inverse Problems* 33.12 (2017), p. 124007.
- [27] Tatiana A Bubba et al. “Deep neural networks for inverse problems with pseudodifferential operators: An application to limited-angle tomography”. In: *SIAM* (2021).
- [28] Steven G Worswick et al. “Deep neural network processing of DEER data”. In: *Science advances* 4.8 (2018), eaat5218.
- [29] Peter D. Lax. *Linear Algebra and Its Applications*. Second. Hoboken, NJ: Wiley-Interscience, 2007. ISBN: 9780471751564 0471751561.
- [30] Michael Rozowski et al. “Input layer regularization for magnetic resonance relaxometry biexponential parameter estimation”. In: *Magnetic Resonance in Chemistry* 60.11 (2022), pp. 1076–1086. doi: <https://doi.org/10.1002/mrc.5289>. eprint: <https://analyticalsciencejournals.onlinelibrary.wiley.com/doi/pdf/10.1002/mrc.5289>. URL: <https://analyticalsciencejournals.onlinelibrary.wiley.com/doi/abs/10.1002/mrc.5289>.
- [31] Hau-Tieng Wu et al. “Evaluating physiological dynamics via synchrosqueezing: Prediction of ventilator weaning”. In: *IEEE Transactions on Biomedical Engineering* 61.3 (2013), pp. 736–744.
- [32] Hau-Tieng Wu et al. “Using synchrosqueezing transform to discover breathing dynamics from ECG signals”. In: *Applied and Computational Harmonic Analysis* 36.2 (2014), pp. 354–359.
- [33] Roberto H Herrera, Jiajun Han, and Mirko van der Baan. “Applications of the synchrosqueezing transform in seismic time-frequency analysis”. In: *Geophysics* 79.3 (2014), pp. V55–V64.
- [34] Jean Baptiste Tary et al. “Spectral estimation—What is new? What is next?” In: *Reviews of Geophysics* 52.4 (2014), pp. 723–749.
- [35] Haizhao Yang, Jianfeng Lu, and Lexing Ying. “Crystal image analysis using 2D synchrosqueezed transforms”. In: *Multiscale Modeling & Simulation* 13.4 (2015), pp. 1542–1572.
- [36] Haizhao Yang et al. “Quantitative canvas weave analysis using 2-D synchrosqueezed transforms: Application of time-frequency analysis to art investigation”. In: *IEEE Signal Processing Magazine* 32.4 (2015), pp. 55–63.
- [37] Jianfeng Lu, Benedikt Wirth, and Haizhao Yang. “Combining 2D synchrosqueezed wave packet transform with optimization for crystal image analysis”. In: *Journal of the Mechanics and Physics of Solids* 89 (2016), pp. 194–210.
- [38] Haizhao Yang. “Synchrosqueezed wave packet transforms and diffeomorphism based spectral analysis for 1D general mode decompositions”. In: *Applied and Computational Harmonic Analysis* 39.1 (2015), pp. 33–66.
- [39] Rok Cestnik and Markus Abel. “Inferring the dynamics of oscillatory systems using recurrent neural networks”. In: *Chaos: An Interdisciplinary Journal of Nonlinear Science* 29.6 (2019), p. 063128.
- [40] Richard G. Spencer and Chuan Bi. “A Tutorial Introduction to Inverse Problems in Magnetic Resonance”. In: *NMR in Biomedicine* 33.12 (2020). e4315 nbm.4315, e4315. doi: <https://doi.org/10.1002/nbm.4315>. eprint: <https://analyticalsciencejournals.onlinelibrary.wiley.com/doi/pdf/10.1002/nbm.4315>. URL: <https://analyticalsciencejournals.onlinelibrary.wiley.com/doi/abs/10.1002/nbm.4315>.
- [41] Chuan Bi et al. “Stabilization of parameter estimates from multiexponential decay through extension into higher dimensions”. In: *Scientific reports* 12.1 (2022), pp. 1–16.
- [42] Richard Spencer et al. “Breaking the CRLB Barrier: Decreasing Mean Squared Error in Parameter Estimation Through Introduction of Regularization Bias”. In: *Bulletin of the American Physical Society* (2022).
- [43] Zhaodi Zhang et al. “Provably tightest linear approximation for robustness verification of sigmoid-like neural networks”. In: *arXiv preprint arXiv:2208.09872* (2022).
- [44] Nasim Rahaman et al. “On the spectral bias of neural networks”. In: *International Conference on Machine Learning*. PMLR. 2019, pp. 5301–5310.
- [45] Nikunj Saunshi et al. “Understanding Influence Functions and Datamodels via Harmonic Analysis”. In: *arXiv preprint arXiv:2210.01072* (2022).

- [46] Maithra Raghu et al. “On the expressive power of deep neural networks”. In: *international conference on machine learning*. PMLR. 2017, pp. 2847–2854.
- [47] Lloyd N Trefethen. *Spectral methods in MATLAB*. SIAM, 2000.

DEPARTMENT OF MATHEMATICS, UNIVERSITY OF MARYLAND, COLLEGE PARK

NATIONAL INSTITUTE ON AGING, NATIONAL INSTITUTES OF HEALTH

DEPARTMENT OF MATHEMATICS, UNIVERSITY OF MARYLAND, COLLEGE PARK